Indian Journal of Experimental Biology
Vol. 61, April 2023, pp. 235-243
DOI: 10.56042/ijeb.v61i04.174

Graphene monolayer as an appropriate substrate for mesenchymal stem cells support in regenerative medicine

Iwona Lasocka[1]*, Ewa Skibniewska[1], Michał Skibniewski[2]*, Lidia Szulc-Dąbrowska[3], Elżbieta Jastrzębska[4], Iwona Pasternak[5], Sitek Jakub[5] & Marie Hubalek-Kalbacova[6,7]

[1]Department of Biology of Animal Environment, Faculty of Animal Science, Warsaw University of Life Sciences, Warsaw, Poland

[2]Department of Morphological Sciences; [3]Department of Preclinical Sciences, Faculty of Veterinary Medicine, Warsaw University of Life Sciences, Warsaw, Poland

[4]Chair of Medical Biotechnology, Faculty of Chemistry, Warsaw University of Technology, Poland

[5]Faculty of Physics, Warsaw University of Technology, Warsaw, Poland

[6]Institute of Pathological Physiology, 1st Faculty of Medicine, Charles University, Prague, Czech Republic

[7]Faculty of Health Studies, Technical University of Liberec, Liberec, Czech Republic

Received 27 September 2022; *revised 28 February 2023*

Synergistic effect of mesenchymal stem cells (MSCs) and graphene monolayer is still a less discussed topic but crucial in the context of creating a graphene skin dressing. Moreover, capturing early changes in the cytoskeleton may prove to be a valuable indicator of cell condition after direct contact with the biomaterial. In this context, here, we investigated the response of human bone marrow mesenchymal stem cells (hBM-MSCs) to graphene monolayer as a scaffold, based on cytoskeleton architecture. Three main components of the cytoskeleton — microfilaments, intermediate filaments and microtubules were characterized as well as analyzed its entire cell morphology (focal adhesions). Based on microscopic analysis and cell area measurements, it can be stated that graphene did not cause a damage or disturbance of any cytoskeleton members and linker proteins (plectin, vinculin) and gap junction protein (connexin 43). hBM-MSCs growing on the graphene monolayer were more spread than cells growing on the glass but without any other significant difference. This suggested that graphene substrate as a monolayer could be a structural reinforcement for MSCs cultivation without affecting their cytoskeleton, which determines cell integrity, connections and migration, all important cell properties in the process of skin wound healing.

Keywords: Connexin 43, Focal contacts, Intermediate filaments, Microfilaments, Microtubules, Plectin

Mesenchymal stem cells (MSCs) have become an attractive cell source for a new generation of cell-based regenerative therapies[1]. The main properties that give MSCs an advantage over other cells are immunomodulatory, self-renewal and differentiation potential. The therapeutic effects of MSCs are attributed primarily to paracrine properties of MSCs including release of extracellular vesicles, bioactive compounds and regulatory substrates[1-3]. Graphene possesses unique properties for biological purpose, like chemical inertness, high elasticity, flexibility, and high thermal conductivity and thus can be used as a perfect scaffold for cell culture[2,4]. Moreover it has been shown that graphene possess antibacterial, antiviral and immunomodulatory properties[2,5]. Material engineering (e.g. preparation of graphene monolayer scaffold) could be used to control MSCs growth and differentiation into functional phenotypes[2,6]. This innovative form of action could bring benefits in regenerative medicine and wound healing treatment.

Nevertheless, surface chemistry, nanotopography and production methods of graphene are important determinants of its cytocompatibility and could cause various cellular responses[2,7]. Therefore, research must be carried out with the use of precisely known material in term of its characteristics[8], which provokes response from cells growing on its surface. Graphene monolayer as a scaffold for cells is poorly known, but its action potential is enormous and gradually confirmed[9-12]. However most of the publications consider graphene flakes or sheets suspended in culture medium[5,12,13]. These two physical forms of graphene: monolayer *versus* flakes/sheets act on cells differently: from the stimulation of wound healing

*Correspondence:
E-Mail: iwona_lasocka@sggw.edu.pl (IL);
michal_skibniewski@sggw.edu.pl (MS)

effects of the graphene monolayer[11] to cytotoxicity due to the contact with the graphene flakes/sheets suspended in the solution[13].

The cytoskeleton plays an important role in mechanosensing and mechanotransduction[11,14]. Environmental changes (e.g. graphene monolayer) are perceived by cells, which can respond to them by changing their morphology and physiologic pathways. The interactions between cell cytoskeleton and a surface onto which cells are attached generate mechanical forces and influence cell shape, proliferation, and differentiation[9,11,14,15].

Further, the reaction of cell in response to environmental stress — substrate surface topography, manifests itself in formation of pronounced actin stress fibers, distinctive microtubules or modification of existing ones, resulting in changes in cell adhesion and spreading. Different research groups demonstrated that seeding density of MSCs is important and had impact on their behaviour, affected cell shape, area of cell spreading and modulated their differentiation and showed that high confluence is detrimental to MSCs quality[16,17].

In the present study, we investigated the response of MSCs to graphene monolayer as a substrate/ scaffold based on cytoskeleton architecture of MSCs, taking into account the seeding density of cells at which the probability of cell-cell contact is low. Synergistic effect of MSCs and graphene is an undiscovered topic and important in the context of creating a graphene skin dressing. Moreover, capturing early changes in the cytoskeleton may prove to be a valuable indicator of cell conditions and futher fate after direct contact with the biomaterial. Hence, we focused on depiction of microfilaments, intermediate filaments (IFs) and microtubules as well as different linker proteins (e.g. plectin and vinculin) and connexin 43 to evaluate their morphology as a hallmark of graphene-based changes in the cell behaviour.

Materials and Methods

Material

Production of graphene was conducted by chemical vapor deposition (CVD). The graphene was grown on copper substrate, and then was transferred onto rounded glass cover using method of electrochemical delamination[18]. Cover slides coated with graphene were treated with alcohol for 30 min and placed into wells of a 24-well plate. The quality of each preparation was certified, by measuring Raman spectrum (UV-Visible-NIR inVia, Renishaw) with characteristic peaks marked (Fig. 1A). The surface morphology of graphene samples was investigated by high-resolution scanning electron microscopy (SEM) Hitachi SU8230 Cold-FEG equipped with a semi-in-lens type objective lens (Fig. 1B). The observations were performed in low voltage range (from 0.5 to 1 kV) to obtain highly topographical information and simultaneously in deceleration mode to improve resolution of the visualization of fine microstructure details.

Cell culture

Human bone marrow mesenchymal stem cells (hBM-MSCs) (Thermo Fisher Scientific) were cultured in low glucose DMEM (Dulbecco's Modified Eagle's Medium, HyClone, USA) supplemented with 10% fetal bovine serum (FBS; Sigma-Aldrich) and 1% antibiotic solution containing 100 U/mL penicillin and 100 µg/mL streptomycin (Sigma-Aldrich) at 37°C in a 5% CO_2 humidified atmosphere.

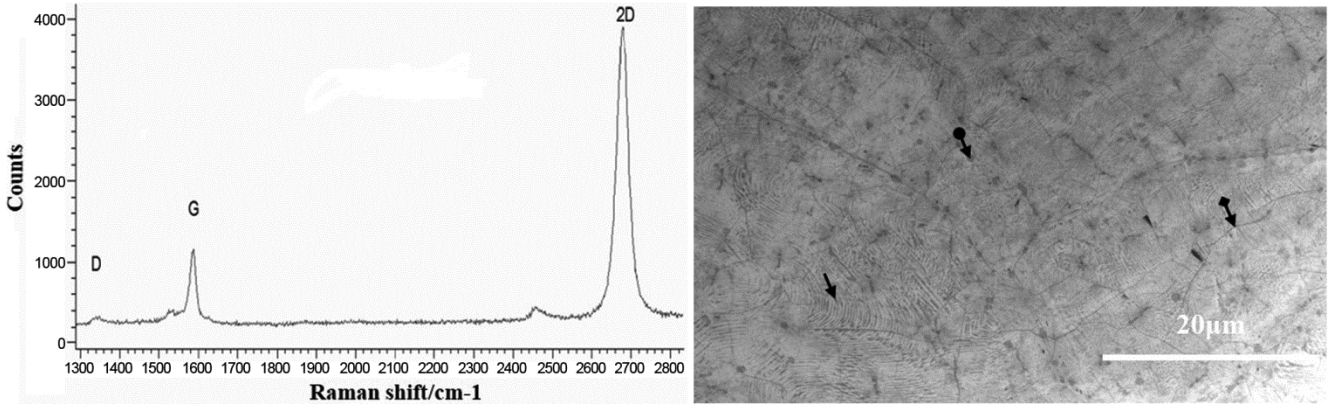

Fig. 1 — Characterization of graphene by (A) Raman spectroscopy; and (B) Scanning electron microscopy (SEM). [The arrows show wrinkles, add layers (arrow with the circle at the beginning) and cracks (arrow with the square at the beginning)]

Passages <7 MSCs were seeded atop sterile microscopic glass coverslips (control) and graphene-coated glass coverslips placed in 24-well plates (Falcon, USA) in density 5×10^2/well. After 48 h, cells were evaluated under microscope, fixed and stained.

Cell morphology

Morphology of living hBM-MSCs was observed after 3 and 48 h of seeding on control or graphene-coated microscopic slides. Images were captured with an inverted microscope (Olympus IX71) equipped with Color View III cooled CCD camera and Cell^F software (Soft Imaging System) (Olympus, Japan). Cell shapes were presented based on vimentin staining.

Cell area calculation

Spread area analysis was performed using ImageJ. About 50-60 living cells were manually outlined and projected cell area was calculated.

Cytoskeleton, FAs protein and GJ protein visualization

hBM-MSCs were fixed with a 4% paraformaldehyde (PFA, Sigma-Aldrich) in PBS for 20 min for F-actin, vinculin, vimentin and plectin staining. For α-tubulin detection, cells were fixed with ice-cold 100% methanol for 2 min. Then the cells were permeabilized with 0.5% Triton X-100 (Sigma-Aldrich) in PHEM buffer and blocked with 2% bovine serum albumin (BSA, Sigma-Aldrich) in PHEM-Triton X-100 (0.1%). Later, the cells were stained with fluorescein isothiocyanate (FITC)-conjugated phalloidin (Sigma-Aldrich) for 20 min. or with primary antibodies (Abs) directed against α-tubulin, vinculin, connexin 43, vimentin and plectin (all from Sigma-Aldrich) for 30 min followed by appropriate secondary Abs: donkey anti-mouse IgG or goat anti-rabbit IgG conjugated with FITC or rhodamine Red-X or Alexa Fluor 568 for 30 min. DNA was stained with 1 μg/mL DAPI or Hoechst 33342 (Sigma-Aldrich) for 2.5 min. Slides were mounted in ProLong Gold Antifade Reagent (Invitrogen, USA) and examined using a fluorescence microscope Olympus BX60 equipped with Color View III cooled CCD camera. Images were analyzed using Cell^F and ImageJ software.

Statistical methods

Three independent experiments were performed in duplicate. Results were expressed as mean ± standard deviation (SD). Statistica 13.3™ (TIBCO) software and based upon the one-way analysis of variance (ANOVA) with post-hoc Tukey's tests were used for statistical analysis. The differences were considered significant from $P \leq 0.05$.

Results

Graphene is known to copy the physical properties of underneath surface e.g. roughness, stiffness[9]. Thus we performRaman spectroscopy method and SEM to characterize the morphology and quality of graphene monolayer (Fig. 1). The preferential defects (wrinkles, add layers and cracks) were confirmed by SEM analysis (Fig. 1B).

In this study, hBM-MSCs were cultivated on graphene monolayer 2D scaffold deposited on a glass coverslip and its influence on these cells was characterized by observing their overall morphology, different cytoskeleton structures and FAs.

Morphology and cell area

After seeding of hBM-MSCs, duomorphic appearance of these cells was noticed: spindle-shape cells or polygonal/flat cells with visible nuclei and some granules in the cytoplasm. Some cells were arranged next to each other, others individually scattered (Fig. 2). Three hours after seeding the cells were already attached to the substrates, becoming well-spread and formation of filopodia started (Fig. 2A). During the following hours, front-back polarity of most of the cells appeared. Summarizing the hBM-MSCs morphological features — the cells changed from round-oval shape, which dominated after 3 h after cell seeding, to elongated or multiform cells after another 45 h of cultivation on the glass and the graphene substrate (Fig. 2B).

Intermediate filaments (IFs) play an important role in mechanotransduction and appear to be relatively stable structures. Thus, vimentin staining was used for visualization of the general cell morphology (shape) (Fig. 2C) and in more detail for determination of its delicate structure. IFs extending towards the cell periphery and delicate network of thread-like filaments, without any abnormalities and interruptions in their arrangement clearly visible (Fig. 2D). hBM-MSCs on the graphene monolayer were slightly larger than on glass (mean: 6025±2877 versus 5989±2983 μm² and median: 5227 *versus* 5011 μm²), respectively. However, when the cells were in contact with each other (Fig. 2E), their surface spreading area was restricted, and in comparison to solitaire cells their area was smaller as well. This phenomenon was noted on both tested surfaces — the graphene and the glass substrate.

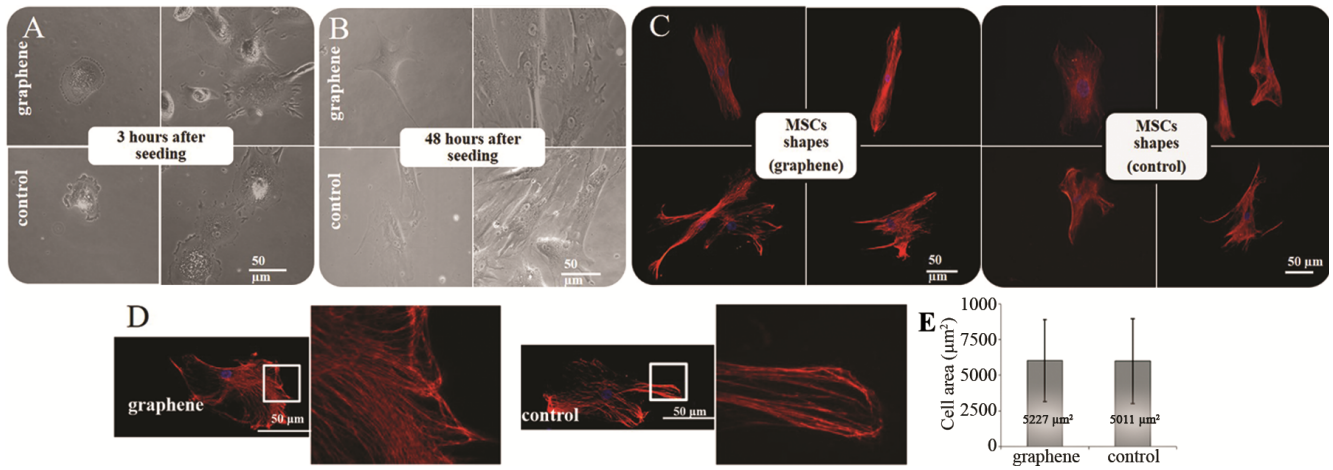

Fig. 2 — Morphology of hBM-MSCs seeding on graphene and glass substrate for (A and B) 3 and 48 h; (C) Shapes of hBM-MSCs seeding on graphene and glass substrate after 48 h (vimentin staining – red fluorescence, DNA staining – blue fluorescence); (D) Distribution of vimentin filament intermediates of hBM-MSCs on graphene and glass substrate. The boxed area corresponds to the magnified view shown on the right; and (E) Effect of graphene on hBM-MSC area. [Data are represented as mean ± SD and median value inside the columns]

Cytoskeleton, FA and GJ protein

The visualization of microfilaments by actin staining (Fig. 3) shows that actin cytoskeleton did not show morphology abnormalities during hBM-MSCs cultivation on the graphene monolayer substrate. As shown in the Fig. 3, the cells, which were more flat and polygonal display thick but not strictly oriented stress fibers both on the graphene monolayer and on the glass substrates. In contrast, well-aligned stress fibers were noted in the spindle shaped cells. These cells have thick stress fibers aligned along the major cell axis. Stress fibers are composed of dorsal stress fibers, which are anchored to focal adhesions at the leading edge of cell, transverse actin arcs, ventral stress fibers and perinuclear actin fibers, which are located above the nucleus. All these mentioned structures were distinguished in hBM-MSCs (Fig. 3). Additionally, we also studied focal adhesions (FAs) which mediate the contact with the substrate and are important in mechanotransduction. Vinculin is one of the proteins contained in FAs (adhesome) linking integrins to actin filaments and its expression allows to specify the strength of cell's interaction with the ground substrate[11]. Activated, for example by talin binding, vinculin interacts with actin filaments and the force transduction is generated in response to environmental stimuli[19]. Vinculin localization in streak-shaped focal adhesions was noted at the cellular periphery (Fig. 3C) and its distribution supports stabilization (anchorage) of the adhesion. On the other hand, its high expression was detectable also in the center of the cell but in diffused form (Fig. 3), because vinculin is present in the whole cytoplasm and only during cell movement concentrated/localized in FAs. Vinculin-positive FAs numbers per cell were calculated and dot and dash adhesions shape were shown (Fig. 3D). There was no difference in numbers of FAs between MSCs growing on graphene monolayer and glass substrate.

Connexin 43 (Cx43) is a transmembrane protein that allows the exchange of biological information between cells which are physically connected and also between separated cells[20]. Representative images of Cx43 distribution in the MSCs cultured on the graphene monolayer and the glass are shown in Fig. 4. This analysis, both on the graphene coated and non-coated glass, revealed intensive expression of Cx43, which was visualized in the cytoplasm and cell membrane but not in the form of typical placoids. Rather, it was distinguished by fine granular cytoplasmic staining with no readily observed membrane-associated plaques. It must be underlined that the detected expression of Cx43 does not definitely indicate the formation of functional active gap junctions between the adjacent MSCs.

Plectin was evenly distributed in the hBM-MSC and also colocalized with actin stress fibers (Fig. 5). No disruptions or gaps in the plectin cell expression were present. Moreover, this protein was abundantly expressed in every cell. Microtubules, the third principal component of cytoskeleton, are found throughout the cell cytoplasm (Fig. 5D). They start

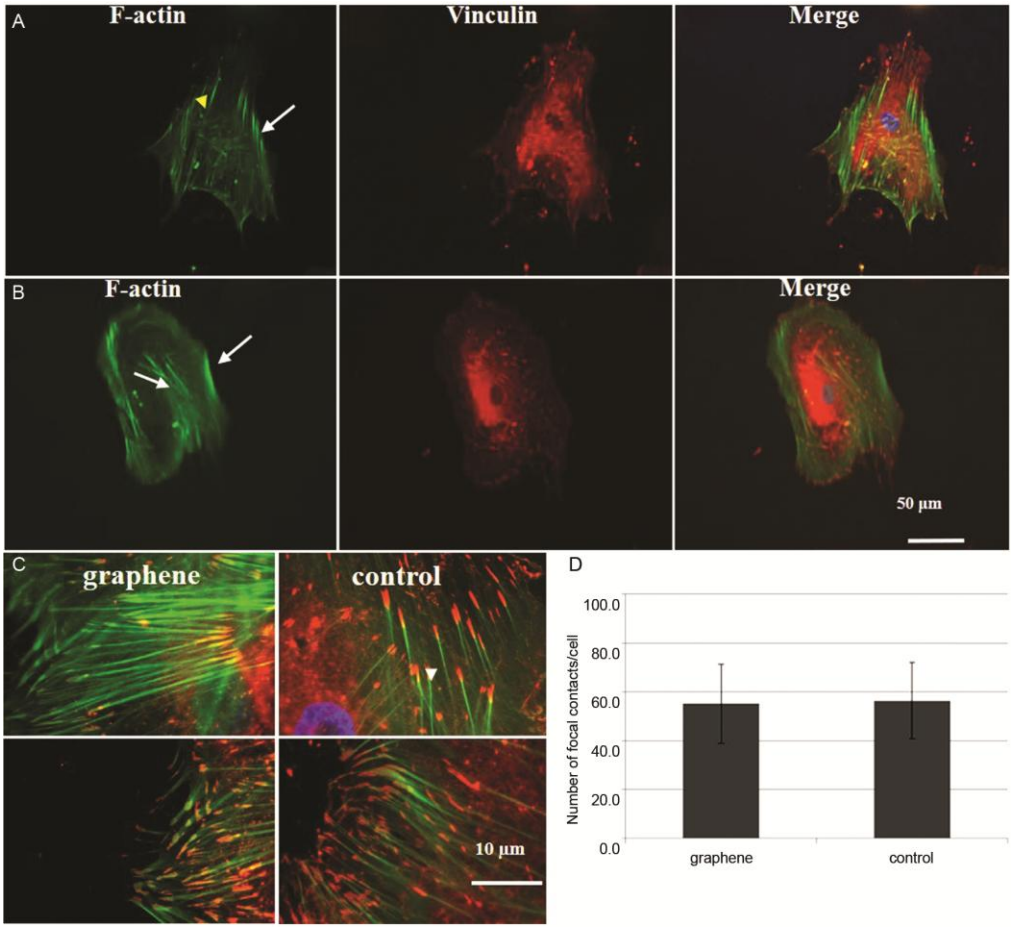

Fig. 3 —Influence of (A-C) graphene and glass as a control on F-actin; and vinculin localization and the interaction between F-actin and vinculin in hBM-MSCs; and (D) Number of focal contacts per cell with no differences between graphene and glass substrates. [The arrows indicate stress fiber network. Yellow arrowhead indicate transverse actin arc. On the upper C images perinuclear actin fibers (white arrowhead) and ventral stress fibers are seen and on the lower dorsal stress fibers, which are anchored to focal adhesions at the cell leading edge, are presented. No cortical disruption of actin was noted. Vinculin distribution in more spread and polygonal cells was abundant along the cell edge, where resembled spikes, but in cells with more spindle shapes vinculin was concentrated on both ends. The magnified images are of the boxed regions and show vinculin at leading and trailing edges of cells. DNA, blue fluorescence]

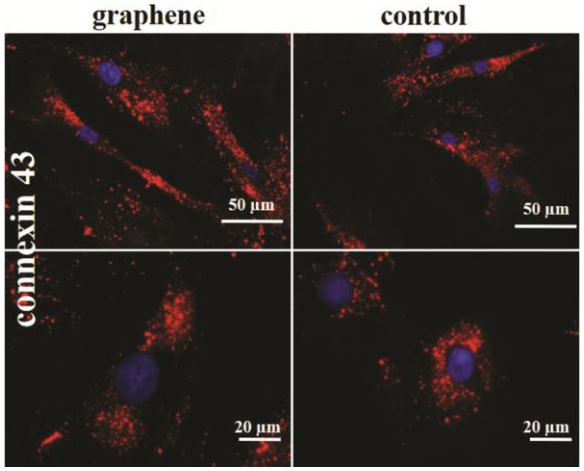

Fig. 4 — Connexin 43 distribution in human bone morrow MSCs growing on (A) graphene substrate; and (B) on the glass. [DNA. blue fluorescence]

out from microtubule organizing center (MTOC) and stretch to the edges of the cell. The integrity of hBM-MSC microtubules on the graphene monolayer platform was maintained and no perturbations of their organization were detected (Fig. 5D).

There were no abnormalities or lack of continuity or mechanical damage in cytoskeleton components of hBM-MSCs growing on the graphene monolayer compare to the glass substrate based on F-actin, vimentin and α-tubulin immunostaining. The direct delivery of MSCs to wounds may induce rapid cell death or disappearance in the blood flow; thus, the introduction of MSCs via graphene nanoscaffolds presents a promising alternative delivery method, which is capable of minimizing unprogrammed cell death and dilution of cells.

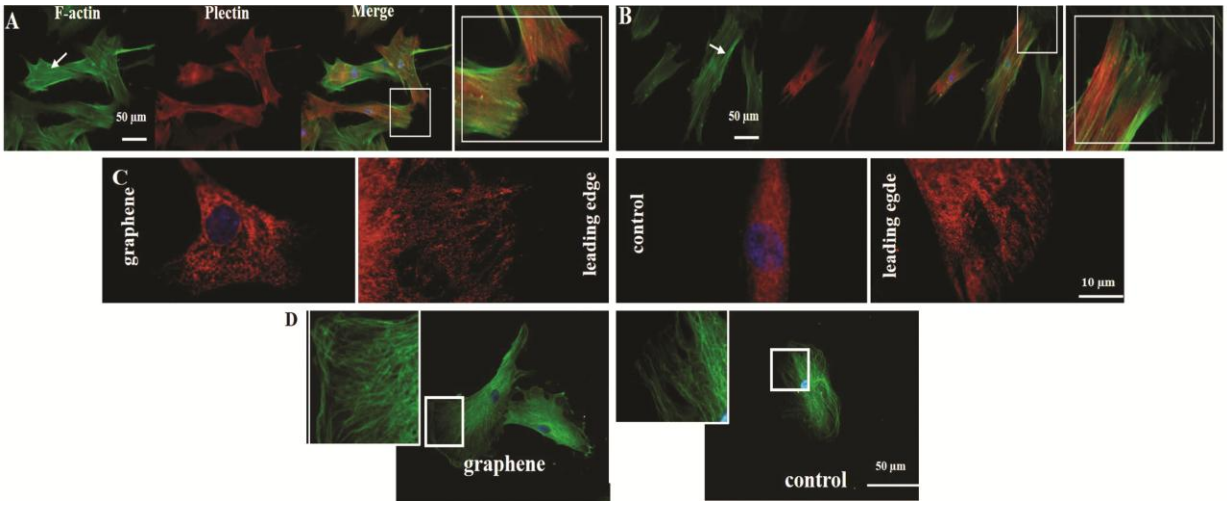

Fig. 5 — Plectin together with F-actin distribution in cells growing on (A) Graphene; and (B) Glass. The magnified images (from A and B) are of the boxed regions and show plectin colocalization with actin stress fibers; (C) Plectin localization in hBM-MSCs and at the leading edge of spread and polygonal cells; and (D) Microtubule filament architecture of hBM-MSCs culturing on graphene scaffold and glass, based on immunofluorescence detection of α-tubulin (green fluorescence). [DNA, blue fluorescence. The magnified images are of the boxed regions. The arrows indicate stress fiber aligned along the major cell axis]

Discussion

Surface properties of materials used as implants or other medical devices have been shown to affect cell growth, shape and the fate of MSCs[15,21-25]. It is thought, that it is related to the topography, stiffness, roughness, wettability, chemistry or energy of these materials. Graphene monolayer used in this work was characterized by the presence of wrinkles, additional layers and cracks. These structures, created during graphene monolayer production, affect cell morphology and may even stimulate cell actiєvity[11,26]. Verdanova *et al.*[27] revealed that wrinkles within graphene monolayer promoted proliferation in osteoblastic cells. A review by Yang *et al.*[24] summarized that surface nanotopography and material stiffness can modulate cell behavior by changing cell adhesion, cell spreading, actin organization, cellular contractility, proliferation, migration speed and cell differentiation. On the other hand Dalby *et al.*[6] suggested that nanomaterials could keep the cells in undifferentiated forms when the adhesive forces are not strong enough (adhesions are not of sufficient size and number).

Well-characterized and homogenous population of MSCs is crucial for therapeutic purposes. hMSCs growing on rough substrate demonstrated spindle, cuboidal and stellate shape. Papageorgiou *et al.*[7] suggested that the last two shapes are representative of morphologies expected for osteoblastic differentiation. Our results confirm this phenomenon, but these shapes mentioned above were noticed on both our tested substrates — graphene monolayer and glass (Fig. 2C). The graphene monolayer is one atom thick, and it mimics the underneath substrate. We have noticed that cells growing on the graphene monolayer (Figs 2, 3 & 5) have elongated body with visible nuclei, filopodia and cellular propagation fronts. Interesting, that area of cells growing on the graphene monolayer was larger than on control glass, based on median value (Fig. 2E). It should be also noted, that some percentage of the cells was much flattened and the value of surface area reached 10×10^3 µm^2 and even more. This mainly concerned single cells without contact with other cells growing on the glass control slide and even on the graphene monolayer (Fig. 3). It may indicate the starting senescence or osteodifferentiation of the MSCs cultivated in our study[28].

Stress fibers are bundles of actin filaments and stiff scaffolds generate more pronounced connections of stress fibers to focal adhesions to resist deformation of cell[29]. They are aligned along the major cell axis in the most animal cell types[30]. This tendency was also noted in our experiments: the elongated MSCs had well-aligned stress fibers and FAs, although more flat and polygonal MSCs did not have so strictly oriented stress fibers. In our experiment, the graphene monolayer had not only any influence on the shape of hBM-MSCs but also on FAs formation (size and number) in comparison to the control glass (Fig. 3).

Dalby *et al*.[6] indicated that adhesion play important role in stem cell fate decision and assigned the extent of intracellular tension, based on cell adhesion formation, for lineage specificity. Large, supermature adhesions and high intracellular tension resulted in osteogenesis. The difference in stress fibers and FAs was more evident in our previous research on fibroblasts L929[11], which is a terminally differentiated cell line than in the primary undifferentiated MSCs. Dalby *et al*.[6] noted that MSCs as well as fibroblasts are intermediate tension phenotypes, and there is only very subtle adhesion differences between them: MSCs have lower intracellular tension and adhere to the matrix more weakly than fibroblasts. Kim *et al*.[10] noted that the use of graphene monolayer enhanced the formation of FAs in adipose-derived hMSCs comparing them to the cells on the glass substrate: about 150 and 100 FAs/cells after 7 days of culturing, respectively. Moreover, authors showed enhanced expression of the connexin 43 in hMSCs growing on the graphene compared to glass and concluded that high quality graphene enhanced cell-substrate and cell-cell interactions.

Connexins (CXs) are gap junction proteins and the most ubiquitously expressed type of Cxs in the skin is connexin 43[31]. Cx43 integrates multiple signals to regulate wound healing, including remodeling of the extracellular matrix, epidermal/dermal cell proliferation and migration, inflammatory response and angiogenesis[31]. Sustained inhibition of Cx43 could have therapeutic potential in normal and chronic wound healing. Dyce *et al*.[32] revealed that Cx43 is important for maintaining an undifferentiated pluripotent population of skin-derived stem cells and that the absence of Cx43 in knockout stem cells mice reduced the rate of cellular migration. As Zhang & Cui[31] summarized non-toxic Cx43 specific inhibitors may also be effective for the treatment of wounds. In our analysis of Cx43, based on immunofluorescence images, expression of Cx43 seemed to be comparable in MSCs growing on graphene coated glass and on the glass substrate (Fig. 4). It should be noted that in Kim'e *et al*.[10], hMSCs were seeded in concentration (4×10^4 cells/sample) and cultured for 7 days so interactions cell-substrate and cell-cell could be different in comaprison to our analysis taken after 48 h and with seeding density of 3×10^2 cell/cm^2.

In various cells of mesenchymal origin distribution and organization of intermediate filaments (IFs) represented by vimentin staining depend on microtubules as well as intact actin cytoskeleton[33]. IFs have high tensile strength and protect cells against mechanical stress[34]. They play a role in maintenance of cell shape and migration[35-37]. IFs can be additionally stabilized by accessory proteins. One of them is plectin, a giant protein, which forms a link between actin filaments, microtubules and intermediate filaments[22,24,25,34,36,38,39]. The ability of plectin to form cross-connections is essential to cope with mechanical stress[36]. The mutations in the human plectin gene (PLEC) cause a variety of rare human disorders: *epidermolysis bullosa simplex* with muscular dystrophy (EBS-MD), EBS-MD with myasthenic features (EBS-MD-MyS), limb girdle muscular dystrophy type 2Q, EBS with pyloric atresia (EBS-PA), and the EBS-Ogna[36,39]. There was shown that actin cytoskeleton and IF network in cells affects each other subcellular localization: actomyosin arc disruption leads to IF network spreading toward the cell edge[34]. Moreover, authors indicate that plectin (a linker protein) is required for interactions between contractile actomyosin arcs and vimentin filaments. Depletion of this protein leads to similar abnormalities compared to vimentin depletion, like impaired cell migration and pronounced stress fibers-attached focal adhesions. Our results showed no anomaly in architecture of the hBM-MSCs cytoskeleton and in the formation of focal adhesions and plectin expression on the graphene substrate. Other authors also pointed that plectin deficiency besides favours stress fiber formation also reduces microtubules (MT) dynamics[38].

Microtubules together with microfilaments and intermediate filaments generate a force that opposes the resistance of the substrate and resist excessive cell deformation, e.g. during cell migration or contact with a stiff and rigid substrate[37,40,41]. Microtubule structure in hBM-MSCs is spindle-like network[42]. In our experiments, α-tubulin was expressed in a typical pattern for hMSCs. It was distributed uniformly in the cytoplasm and microtubule networks were maintained. There were no differences in microtubule distribution and structure in hMSCs culturing on the graphene and on the glass substrates. However, Duan *et al*.[13] revealed that pristine and oxidized graphene nanosheets are toxic to A549 and Raw264.7 cells. Electron micrographs showed pores formation on both cell membranes. In our opinion physical form (in suspension) of graphene (for example: sheets, flakes,

powder or monolayer covering) affects cells in different way: from toxic effects to positive stimulation. However, graphene monolayer scaffold used in our research is non-toxic for hBM-MSCs and cause no damage to cytoskeleton structure (Figs 1-3 & 5). Given that the graphene substrate used in the study does not adversely affect the structures of the cell's cytoskeleton, it can be expected that this material will find application as a scaffold in tissue regeneration, on which cells can be placed to accelerate the wound healing process. Graphene monolayer combined with MSCs could enhance both the wound healing process and infection control at the injury site.

Conclusion

Not all changes in the cell due to the interaction with the material (e.g. graphene monolayer) are reflected in an increase or decrease of cell viability, proliferation or fate. Capturing early changes in the cytoskeleton may prove to be a valuable indicator of cell conditions and their further fate. The graphene monolayer did not cause any damage of any cytoskeleton fibers and any disturbances in cell localization of associated with cytoskeleton proteins: vinculin (focal adhesion), plectin (cytolinker protein) and connexin 43 (gap junction protein). No morphology abnormalities during hBM-MSCs cultivation on the graphene monolayer substrate were detected. This is a further proof of the lack of cytotoxic effect of the graphene monolayer as a scaffold for cells. Using the beneficial properties of graphene and its scaffold-support function for stem cells may become a breakthrough in biotechnology and regenerative medicine by applying them together to accelerate wound healing.

Acknowledgement

This work was supported by the Scholarship Fund (Grant number: 505-10-072500-P00191-99) of the Warsaw University of Life Sciences (SGGW).

References

1 Fan XL, Zhang Y, Li X & Fu OL, Mechanisms underlying the protective effects of mesenchymal stem cell-based therapy. *Cell Mol Life Sci*, 77 (2020) 2771.

2 Lasocka I, Jastrzębska E, Szulc-Dąbrowska L, Skibniewski M, Pasternak I, Kalbacova MH & Skibniewska EM, The effects of graphene and mesenchymal stem cells in cutaneous wound healing and their putative action mechanism. *Int J Nanomed*, 14 (2019) 2281.

3 Lukomska B, Stanaszek L, Zuba-Surma E, Legosz P, Sarzynska S & Drela K, Challenges and Controversies in Human Mesenchymal Stem Cell Therapy. *Stem Cells Int*, (2019) 9628536.

4 Bellet P, Gasparotto M, Pressi S, Fortunato A, Scapin G, Mba M, Menna E & Filippini F, Graphene-Based Scaffolds for Regenerative Medicine. *Nanomaterials* (*Basel*), 5 (2021) 404.

5 Hashmi A, Nayak V, Singh KRB, Jain B, Baid M, Alexis F & Singh AK, Potentialities of graphene and its allied derivatives to combat against SARS-CoV-2 infection. *Mater Today Adv*, 13 (2022) 100208.

6 Dalby MJ, Garcia A & Salmeron-Sanchez M, Receptor control in mesenchymal stem cell engineering. *Nat Rev Mater*, 3 (2018) 1.

7 Papageorgiou DG, Kinloch IA & Young RJ, Mechanical properties of graphene and graphene-based nanocomposites. *Prog Mat Sci*, 90 (2017) 75.

8 Arthisreea D, Joshib GM & Madhuria W. Photosensitivity of Graphene Quantum Dots Dispersed Polyvinyl Butyral Nanocomposites. *Indian J Pure Appl Phys*, 59 (2021) 775.

9 Hubalek Kalbacova M, Verdanova M, Broz A, Vetushka A, Fejfar A & Kalbac M, Modulated surface of single-layer graphene controls cell behavior. *Carbon*, 72 (2014) 207.

10 Kim J, Park S, Kim YJ, Jeon CS, Lim KT, Seonwoo H, Cho SP, Chung TD, Choung P-H, Choung Y-H, Hong BH & Chung JH, Monolayer graphene-directed growth and neuronal differentiation of mesenchymal stem cells. *J Biomed Nanotechnol*, 11 (2015) 1.

11 Lasocka I, Szulc-Dabrowska L, Skibniewski M, Skibniewska E, Strupinski W, Pasternak I, Kmiec H & Kowalczyk P, Biocompatibility of pristine graphene monolayer: Scaffold for fibroblasts. *Toxicol In Vitro*, 48 (2018) 276.

12 Lasocka I, Szulc-Dąbrowska L, Skibniewski M, Skibniewska E, Gregorczyk-Zboroch K, Pasternak I & Hubalek Kalbacova M, Cytocompatibility of Graphene Monolayer and Its Impact on Focal Cell Adhesion, Mitochondrial Morphology and Activity in BALB/3T3 Fibroblasts. *Materials*, 14 (2021) 643.

13 Duan G, Zhang Y, Luan B, Weber JK, Zhou RW, Yang Z, Zhao L, Xu J, Luo J & Zhou R, Graphene-Induced Pore Formation on Cell Membranes. *Sci Rep*, 7 (2017) 42767.

14 Trubelja A & Bao G, Molecular mechanisms of mechano-sensing and mechanotransduction. *Extreme Mech Lett*, 20 (2018) 91.

15 Ambriz X, de Lanerolle P & Ambrosio JR, The Mechanobiology of the Actin Cytoskeleton in Stem Cells during Differentiation and Interaction with Biomaterials. *Stem Cells Int*, (2018) 2891957.

16 Balint R, Richardson SM & Cartmell SH, Low-density subculture: a technical note on the importance of avoiding cell-to-cell contact during mesenchymal stromal cell expansion. *J Tissue Eng Regenerative Med*, 9 (2015) 1200.

17 Banik BL, Riley TR, Platt CJ & Brown JL, Human mesenchymal stem cell morphology and migration on microtextured titanium. *Front Bioeng Biotechnol*, 4 (2016) 41.

18 Ciuk T, Pasternak I, Krajewska A, Sobieski J, Caban P, Szmidt J & Strupinski W, Properties of Chemical Vapor Deposition Graphene Transferred by High-Speed

Electrochemical Delamination. *J Phys Chemi C*, 117 (2013) 20833.

19 Frank V, Kaufmann S, Wright R, Horn P, Yoshikawa HY, Wuchter P & Tanaka M, Frequent mechanical stress suppresses proliferation of mesenchymal stem cells from human bone marrow without loss of multipotency. *Sci Rep*, 6 (2016) 24264.

20 Ribeiro-Rodrigues TM, Martins-Marques T, Morel S, Kwak BR & Girão H, Role of connexin 43 in different forms of intercellular communication - gap junctions, extracellular vesicles and tunnelling nanotubes. *J Cell Sci*, 21 (2017) 3619.

21 Ghasemi L, Prabhakaran M, Lingling T, Shamirzaei-Jeshvaghani E, Dehghani L & Ramakrishna S, Structural properties of scaffolds: Crucial parameters towards stem cells differentiation. *World J Stem Cells*, 7 (2015) 728.

22 Boyan BD, Cheng A, Olivares-Navarrete R & Schwartz Z, Implant Surface Design Regulates Mesenchymal Stem Cell Differentiation and Maturation. *Adv Dent Res*, 1 (2016) 10.

23 Ghensi P, Bressan E, Gardin C, Ferroni L, Soldini MC, Mandelli F, Soldini C & Zavam B, The biological properties of OGI surface positively act on osteogenic and angiogenic commitment of mesenchymal stem cells. *Materials*, 10 (2017) 1321.

24 Yang Y, Wang K, Gu X & Leong KW, Biophysical Regulation of Cell Behavior—Cross Talk between Substrate Stiffness and Nanotopography. *Engineering (Beijing)*, 3 (2017) 36.

25 Chen M, Sun Y, Hou Y, Luo Z, Li Z, Wei Y, Chen M, Tan L, Cai K & Hu Y, Constructions of ROS-responsive titanium-hydroxyapatite implant for mesenchymal stem cell recruitment in peri-implant space and bone formation in osteoporosis microenvironment. *Bioact Mater*, 18 (2022) 56.

26 Lasocka I, Jastrzębska E, Zuchowska A, Skibniewska E, Skibniewski M, Szulc-Dąbrowska L, Pasternak I, Sitek J & Hubalek Kalbacova M, Graphene 2D platform is safe and cytocompatibile for HaCaT cells growing under static and dynamic conditions. *Nanotoxicology*, 16 (2022) 610.

27 Verdanova M, Rezek B, Broz A, Egor U, Babchenko O, Artemenko A, Izsák T, Kromka A, Kalbác M & Kalbacova M, Nanocarbon allotropes – graphene and nanocrystalline diamond – promote cell proliferation. *Small*, 12 (2016) 2499.

28 Weng Z, Wang Y, Ouchi T, Liu H, Qiao X, Wu C, Zhao Z, Li L & Li B. Mesenchymal Stem/Stromal Cell Senescence: Hallmarks, Mechanisms, and Combating Strategies. *Stem Cells Transl Med*, 11 (2022) 356.

29 Lee S & Kumar S, Actomyosin stress fiber mechanosensing in 2D and 3D. *F1000 Res*, 5 (2016) 2261.

30 Lehtimäki JI, Rajakylä EK, Tojkander S & Lappalainen P, Generation of stress fibers through myosin-driven reorganization of the actin cortex. *eLife*, 10 (2021) 60710.

31 Zhang XF & Cui X, Connexin 43: key role in the skin. *Biomed Rep*, 6 (2017) 605.

32 Dyce PW, Li D, Barr KJ & Kidder GM, Connexin43 is required for the maintenance of multipotency in skin-derived stem cells. *Stem Cells Dev*, 23 (2014) 1636.

33 van Bodegraven EJ & Etienne-Manneville S, Intermediate Filaments from Tissue Integrity to Single Molecule Mechanics. *Cells*, 10 (2021) 1905.

34 Jiu Y, Peränen J, Schaible N, Cheng F, Eriksson JE, Krishnan R & Lappalainen P, Vimentin intermediate filaments control actin stress fiber assembly through GEF-H1 and RhoA. *J Cell Sci*, 130 (2017) 892.

35 Paulin D, Lilienbaum A, Kardjian S, Agbulut O & Li Z, Vimentin: Regulation and pathogenesis. *Biochimie*, 197 (2022) 96.

36 Pânzaru MC, Caba L, Florea L, Braha EE & Gorduza EV, Epidermolysis Bullosa—A Different Genetic Approach in Correlation with Genetic Heterogeneity. *Diagnostics*, 12 (2022), 1325.

37 Stavenschi E & Hoey DA, Pressure-induced mesenchymal stem cell osteogenesis is dependent on intermediate filament remodeling. *Faseb*, 33 (2019) 4178.

38 Castañón MJ & Wiche G, Identifying Plectin Isoform Functions through Animal Models. *Cells*, 10 (2021) 2453.

39 Wiche G, Plectin-Mediated Intermediate Filament Functions: Why Isoforms Matter. *Cells*, 10 (2021) 2154.

40 Tvorogova A, Saidova A, Smirnova T & Vorobjev I, Dynamic microtubules drive fibroblast spreading. *Biol Open*, 13 (2018) 038968.

41 Park R, Yoon JW, Lee JH, Hong SW & Kim JH, Phenotypic change of mesenchymal stem cells into smooth muscle cells regulated by dynamic cell-surface interactions on patterned arrays of ultrathin graphene oxide substrates. *J Nanobiotechnol*, 20 (2022) 17.

42 Calogero AM, Viganò M, Budelli S, Galimberti D, Fenoglio C, Cartelli D, Lazzari L, Lehenkari P, Canesi M, Giordano R, Cappelletti G & Pezzoli G, Microtubule defects in mesenchymal stromal cells distinguish patients with Progressive Supranuclear Palsy. *J Cell Mol Med*, 22 (2018) 2670.